# Chapter III

# Paper II

# On the effect of a sill on dense water formation in a marginal sea

Doroteaciro Iovino

*Nansen Environmental and Remote Sensing Center, Bergen, Norway*
*Bjerknes Centre for Climate Research, Bergen, Norway*

Fiammetta Straneo and Michael A. Spall

*Woods Hole Oceanographic Institution, Woods Hole, Massachusetts, USA*

submitted to *Journal of Marine Research*, 2007

**ABSTRACT:** The properties of water mass transformation in a semi-enclosed basin subject to surface cooling are analyzed both theoretically and numerically using an ocean general circulation model. A fundamental ingredient in this study is the presence of a sill in the strait connecting the basin to the outer open ocean.

The key process that determines the properties of the water mass formed in the marginal sea is the interaction between the interior of the marginal sea and a boundary current that cyclonically encircles it. This exchange is due to mesoscale eddies, and is controlled by baroclinic instabilities of the boundary current. While the structure of the boundary current and its instability are set by the sloping bottom configuration in the absence of a sill, they are significantly influenced by the sill configuration when it is introduced. This results in important changes in the circulation: waters in the interior and in the outflow become colder; the boundary current into the basin becomes narrower and shallower, limited at the sill depth over the open geostrophic contours. The magnitude of the sill influence is a function of its depth.

The presence of the sill limits the transport of warm inflow and reduces the temperature of the waters in the marginal sea. Theoretical

analysis provides further insight into the dynamics at play: the sill, modifying the horizontal and vertical structure of the boundary current, makes it more unstable, and enhances the exchange of heat with the interior, partly offsetting the cooling due to the blocking.

## 3.1 Introduction

Open ocean convection is thought to be an essential ingredient of the present climate system, and plays an important role in maintaining the global thermohaline circulation (Marotzke 2000; Rahmstorf 2002). Variability in the intensity and location of convection in a few selected regions (the Nordic Seas, the Labrador Sea, and the Weddell Sea) is thought to impact the oceanic transports of heat and volume (IPCC 2001; Rahmstorf 2002). Given the observed increase in the global temperature, there has been great interest in the dynamics of water mass transformation and deep convection at high latitudes since those mechanisms are responsible for the global production of deep water (such as the North Atlantic Deep Water and the Antarctic Bottom Water). This focus has increased our knowledge of how open-ocean convective regions work and improved parameterizations of convection in global models (e.g. Visbeck et al. 1996; LabSea Group 1998; Canuto et al. 2004). For the most part, however, these studies have focused on convection as an isolated process, which occurs in regions that are characterized by weak stratification and are subject to strong winter buoyancy loss to the atmosphere (such as the Greenland Sea, the Labrador Sea, and the northwestern Mediterranean Sea, see Marshall and Schott 1999 for a review). The exchange between the convective region and the surrounding oceanic circulation in some previous studies is implicitly included as restoring boundary conditions but is generally not realistically represented (e.g. Jones and Marshall 1993).

More recently, a number of studies have sought to describe the dense water formation process as one component of a larger setting (Spall 2003; 2004; Straneo 2006b). The new paradigm, introduced in the above mentioned studies, is different since it aims to describe not just the open-ocean convective region but the entire marginal sea/semi-enclosed basin in which convection occurs. In this framework, dense water formation occurs in the interior of a marginal sea that is connected to the open ocean through a narrow strait, and subject to buoyancy loss at the surface (Spall 2004; Straneo 2006b). The source of heat that balances this net annual buoyancy loss is provided by a cyclonic boundary current system that advects buoyant water into the basin and exports dense water

out of it. Heat is supplied from the boundary current to the interior region through eddies that result from instabilities of the boundary current. The interior is, on average, a quiescent region where deep and intermediate convection occurs. The boundary current thus plays a fundamental role in this scenario since its instability is the dominant process regulating the exchange with the interior of the marginal sea. The applicability of this paradigm for the Labrador Sea is supported by the analysis of both historical and modern data (Straneo 2006a).

The studies mentioned above, however, do not include the presence of sills, a topographic feature that is present at the boundary of convecting marginal seas such as the Nordic Seas, the Mediterranean. Sills may have a large impact on the dense water formation process not only because they may influence the exchange between the open ocean and the marginal sea, but also because they may affect the structure of the boundary current in the marginal sea, which has been shown to be a key player in the process. Evidence of the importance of sills is provided by a number of model studies. Roberts and Wood (1997) analyzed the sensitivity of the large-scale circulation in a coarse-resolution ocean model to slight modifications of topography in the Greenland-Scotland Ridge. They found that these changes have a significant impact on the locations of water mass formation and on the transport of dense water over the ridge: deepened passages allow an increase of the poleward heat transport. Walin et al. (2004) consider a basin with two bowl-shaped parts connected over a sill to explore the influence of heat loss on the structure of a warm buoyant current that passes over a sill into the cold northern semi-enclosed basin. In their simulations the flow enters the basin as a baroclinic current with a thickness approximately equal to the sill depth, and is transformed to a barotropic slope current while encircling the basin. They find that the sill depth regulates the volume and heat transports over the sill: a deeper sill results in larger transports.

There is, however, still a need to understand more fundamentally the role of the sill in that class of convective marginal seas that are separated from the major ocean basins by such a topographic feature. The purpose of this study is to extend the theory developed by Spall (2004) and Straneo (2006b) to a marginal sea bound by a sill. In particular, we are interested in determining what influence (if any) the sill has on the properties of the dense water produced within the marginal seas, and on the flows into and out of the basin. To do this we explore the dynamical consequences of the topographic constraint on the marginal sea circulation. We restrict our study to configurations for which the sill is sufficiently deep or the strait sufficiently wide, so that the exchange with

the open ocean is not hydraulically controlled. We approach this problem with a set of numerical experiments as well as with theoretical arguments. An analysis of the proprieties of the water formed in the interior of the basin and of the water exported from the basin for varying sill geometry is presented. The basin configurations are essentially idealized in order to allow for simple representations of geometrical parameters, and to estimate their influences on the quantities of interest.

The paper is structured as follows. Section 2 presents the primitive equation model used in the numerical sensitivity study. A comparison between numerical simulations with and without a sill is presented in section 3. The theoretical issues, used to estimate the proprieties of the water masses as function of the sill configuration, are presented and compared to numerical model results in section 4. A summary and conclusions are presented in section 5.

### 3.2 Numerical model

A set of numerical simulations is carried out with the MIT general circulation model (Marshall et al. 1997a, b) to analyze the thermally driven circulation in an idealized semi-enclosed marginal sea. The model configuration closely follows that used by Spall (2004). The model solves the momentum and density equations on a staggered C-grid in the horizontal and with z coordinates in the vertical. The domain is 1200 km by 1500 km wide and 2200 m deep (Figure 1). The horizontal grid spacing is 10 km, and there are 16 vertical levels with a resolution ranging from 100 m at the surface to 250 m at the bottom. The model retains a free surface, and uses Cartesian coordinates on an *f*-plane, with the Coriolis parameter $f = 10^{-4}$ s$^{-1}$.

Laplacian parameterizations of viscosity and diffusivity are used. Horizontal and vertical viscosities are 100 m$^2$ s$^{-1}$ and $5 \times 10^{-4}$ m$^2$ s$^{-1}$, respectively; whereas horizontal and vertical diffusivities are 50 m$^2$ s$^{-1}$ and $5 \times 10^{-5}$ m$^2$ s$^{-1}$, respectively. No-slip boundary condition is applied, and there are no heat and mass fluxes through the solid boundaries. The time step is 1500 s for both barotropic and baroclinic components.

The density ρ depends linearly on temperature, so that $\rho = \rho_0 - \alpha(T - T_b)$ where $\rho_0$ is the reference density for seawater, $\alpha = 0.2$ kg m$^{-3}$ °C$^{-1}$ is the thermal expansion coefficient, and $T_b = 4$ °C is the initial temperature at the bottom. An annual cycle of sea-surface cooling of 200 W m$^{-2}$ is applied over the marginal sea for 2 months, followed by no forcing for 10 months (the resulting annual mean ocean

heat loss is 33 W $m^{-2}$). Any spatial variability that arises in the solutions is thus a result of lateral advection in the ocean.

Water from the open ocean is supplied to balance the cooling in the marginal sea. This is achieved by restoring the temperature within the dashed rectangle in the open ocean (Figure 1) toward a linear profile $T_0(z) = T_b + k(z_b - z)$, where $z_b$ is the maximum bottom depth and $k = T_0^{'}(z) = 1.5 \times 10^{-3}$ °C $m^{-1}$ the vertical temperature gradient. The initial upper-layer temperature is about 7.2 °C. The relaxation time scale is set to 50 days. In this way, the properties of the water flowing into the marginal sea are essentially fixed, independent of what processes take place in the marginal sea. $T_0(z)$ is also used to set the initial uniform stratification. The internal deformation radius based on this open ocean stratification is on the order of 20 km.

The circular basin is connected to the ocean through a 400km wide strait. The boundaries slope all around the perimeter from 200 m to 2200 m depth over a distance of 140 km, corresponding to a bottom slope of $h_r = 1.43 \times 10^{-2}$. The sill has a meridional extent of 160 km, and is 800m deep in the reference sill-simulation (Figure 1). A unique and important aspect of the basin with a sill is the presence of a region of closed geostrophic contours (i.e., closed contours of constant *f*/H where H the basin depth, CGC) in the interior, and an outer region of open geostrophic contours (OGC) that connect with the open ocean.

A series of experiments are performed that differ only in the strait topography, varying the sill depth from 400 m to 1500 m. This range of sill depths does not result in a hydraulic control of the flow at the strait. Sufficiently narrow straits or shallow sills can cause a hydraulic jump to occur within the strait; however, these configurations will not be accurately represented by the dynamics considered here.

Using this idealized configuration, this study aims at a model formulation that is general and suitable to any marginal sea with similar large-scale characteristics. However, the basin dimensions are roughly corresponding to the Nordic Seas. The heat flux from the surface used in this study is close to the average winter heat flux over the Nordic Seas in the last decades (Blindheim and Østerhus 2005). Obviously this set-up is representative of the Nordic Seas only in a very idealized sense. In particular, the rather complex bathymetry that characterizes the Nordic Seas' interior is neglected. Also, there are no exchanges with the Barents Sea and the Artic Ocean, and only one gateway to the Atlantic Ocean. The basic circulation and governing physics do not appear to be sensitive to variations in the basin dimensions (Spall 2004). Simulations

in a smaller basin of 750 km diameter give results qualitatively similar to the larger basin.

All simulations have been integrated for 35 years. Most of the results presented below represent pentad average fields when a statistical equilibrium is already achieved.

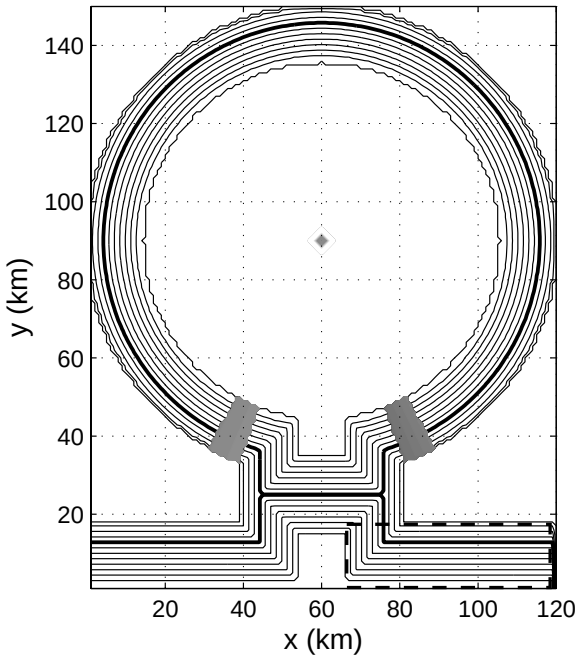


**Figure 1.** Basin configuration used in the numerical simulation with a sill at 800 m. Contour interval is 200 m. The thick black line is the 800m isobath. The dashed rectangle indicates the region where the model temperature is restored. Grey areas are used for calculations shown in Figure 5.

## 3.3 Numerical results

In this section we first describe and compare the qualitative properties of the time-averaged fields of two runs: a basin without sill, essentially reproducing Spall's (2004) simulations, and a basin with an 800m-deep sill (hereafter referred to as NOSILL and SILL, respectively). The results will show that the basic dynamics in SILL are qualitatively similar to the NOSILL reference case, but also that the sill has a significant impact on the characteristics of dense water formation and outflow.

In both simulations the circulation over the sloping topography reaches an equilibrium seasonal cycle in less than a decade. The interior takes longer to reach a steady state: in the beginning it cools because the temperature difference between the interior and sloping-bottom regions is not sufficiently large to generate enough eddies from the boundary current to balance the heat loss over the interior. Notably, the interior in NOSILL takes approximately 15 years to reach the steady state compared to more than 20 years in SILL.

### *3.3.1 NOSILL circulation*

The general features of the circulation in NOSILL are qualitatively similar to those of Spall (2004). The net heat loss over the marginal sea drives a warm inflow from the open ocean, which travels cyclonically around the basin over the sloping topography (Figure 2). The topography around the perimeter of the marginal sea is instrumental in controlling the circulation and the properties of the water masses formed within the basin. The presence of sloping topography sustains the boundary current, which carries warm water into the marginal sea, and, through baroclinic instability, provides eventual restratification of the interior through formation of lateral eddies. Hence, as required to balance the heat budget in the marginal sea, this boundary current cools as it encircles the basin so that the outflow is approximately 0.5 °C colder than the inflow, but warmer than the water masses formed in the interior of the marginal sea. The properties of the outflowing water are determined by the exchanges between the cyclonic boundary current and the interior; this interaction is controlled by baroclinic instabilities of the boundary current. The inner flat-bottom region is characterized by the lowest temperatures, approximately 1 °C colder than the inflow.

The mean vertical structure in the marginal sea shows the contrast between the circulation in the sloping-bottom and flat-bottom regions (Figure 3). The water column is warm and strongly stratified over the sloping boundary where the isotherms are sharply inclined. The boundary current is strong and surface-intensified. The maximum inflow velocity is of about 25 cm $s^{-1}$. The outflow along the western boundary has a slightly higher maximum velocity, and is narrower and deeper than the flow on the eastern side. The velocities in the deep-layers increase around the basin, and the net effect is a barotropization of the flow, in agreement with the theory described in Spall (2004), Walin et al. (2004), and Straneo (2006b). The water column is cold and very weakly stratified over the flat bottom, with stratification increasing slightly in

the upper 100m. The cyclonic circulation in the interior is much weaker with mean velocities of approximately 5 cm $s^{-1}$.

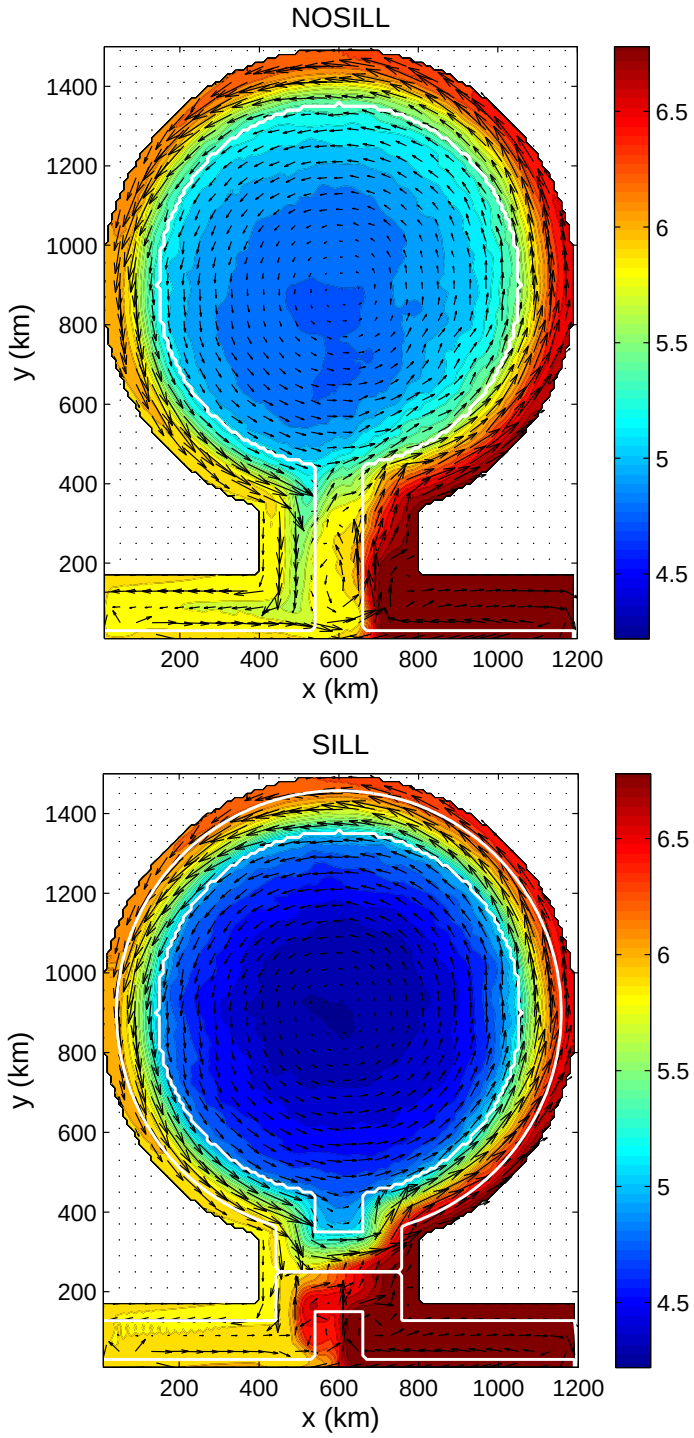


**Figure 2.** Surface temperature (in °C; contour interval is 0.1 °C) and velocity (every fourth grid point), averaged over the last 5 years of

model integration for NOSILL and SILL. White curves bound the flat bottom interior and also the 800m contour in the lower panel.

In NOSILL, the average depth of the boundary current is approximately one-half the depth of the basin, and its average width equal to the width of the sloping boundary, consistent with simulations presented by Spall (2004). Changes in the bottom slope would result in different boundary current structures: wider sloping boundaries and deeper basins enlarge and deepen the boundary current. Therefore, the topographic configuration of the sloping boundaries partly shapes the boundary current, and therefore controls the baroclinic instability.

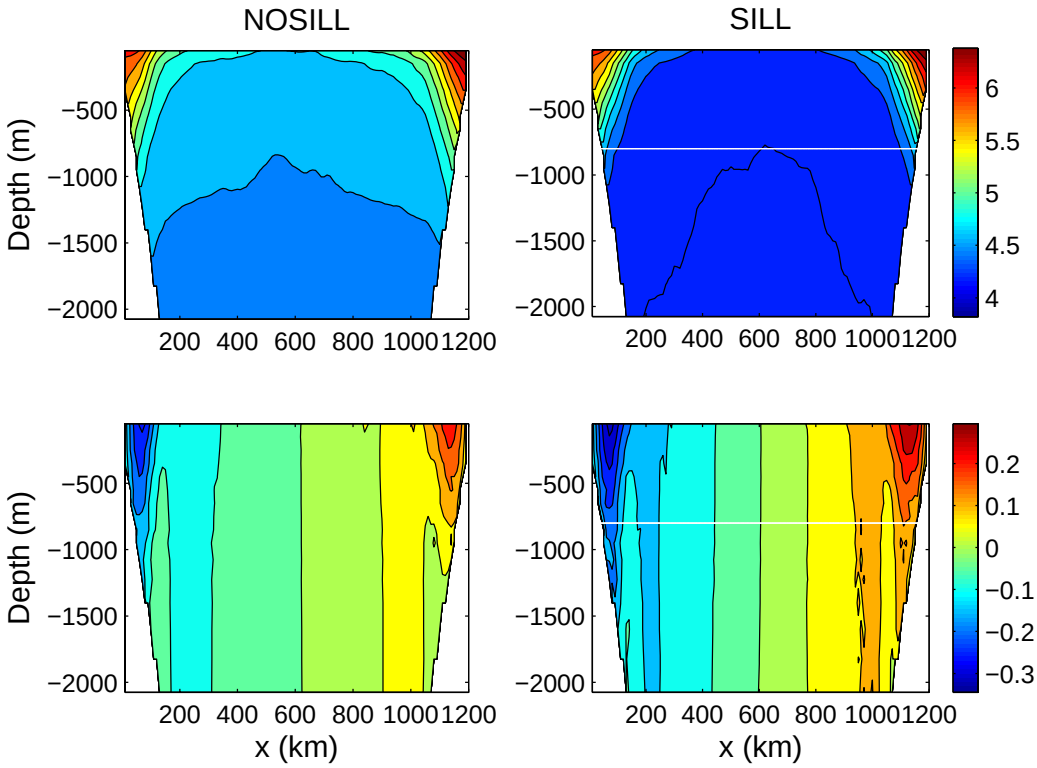


**Figure 3.** Zonal sections at the mid-latitude of the marginal sea: temperature (in °C; upper panels), and meridional velocity (in m $s^{-1}$; lower panels) for NOSILL and SILL. Contour interval is 0.2 °C for the temperature, and 0.05 m $s^{-1}$ for the velocity. White lines indicate sill depth.

### 3.3.2 Changes due to the sill

While qualitatively the SILL experiments exhibit the same dynamics as the basin without sill, the results show that the sill influences the properties of the water masses within the marginal sea. The introduction of the sill at 800m limits the passage of the water in and out of the basin (we will use the term "blocking" to denote this effect due to the sill). The sill introduces some robust changes within the marginal sea. In particular, at the surface there is a significant decrease in the temperatures of the interior and outflowing waters (both about 0.5 °C lower than NOSILL). The inflowing waters are, on average, warmer with a sill because it is only the upper ocean water that can be advected into the marginal sea. The boundary current is narrower. The flow over the seaward side of the sloping topography does not considerably change its temperature as it flows around the basin. Furthermore, the water below sill depth does not exit from the marginal sea, but follows the closed isobaths and re-circulates in the basin (Figures 2).

As a consequence of the blocking effect, the sill strongly impacts the strength and structure of the boundary current by reducing in its width and its vertical extent. The inflow maximum velocity is of about 30 cm $s^{-1}$. The circulation in the interior is almost twice as strong as in NOSILL (Figure 3). In NOSILL, the part of the current that advects heat is as wide as the sloping topography (140 km) and about 1100 m deep. The flow that advects heat in the basin is narrower and shallower in SILL: approximately 80 km wide (slightly wider than the portion of sloping boundaries above the sill) and 800 m deep, the sill depth (Figure 4).

Two regimes can be distinguished over the sloping topography in presence of the sill. The first regime is connected with the OGC. The mean circulation over the open contours is similar to the NOSILL case, but within a thinner area where the temperature decreases, and the velocity becomes more barotropic while the boundary current circles around the basin. A second region is that related to the CGC. Over this region the temperature does not change significantly around the basin, the flow does not contribute to the advection of heat around the marginal sea, and to the exchange of heat with the flat bottom region (Figure 4).

The comparison shown in Figure 4 suggests that the boundary current primarily loses heat over the OGC region. Only the open contours extend from the open-ocean area where temperature is restored, providing a source of heat through the marginal sea. The mean advection along these contours is primarily responsible for balancing the surface cooling in the interior, through the lateral transport of heat by eddies into the CGC and flat bottom regions. Waters outflowing over the sill derive

from the flow over this region (i.e., from layers above the depth of the sill). The region of closed CGC is characterized by a dome of cold water rounded by the cyclonic boundary current. Basin geometries with an associated CGC region in the central part of the domain fundamentally alter the character of the circulation in the basin, creating a trapped cyclonic recirculation over itself. Over the closed contours the mean advection of heat is negligible, and the surface heat flux is balanced by lateral eddy fluxes, which draw heat from the mean advection along OGC and carry it within the interior (Spall 2005). It has to be noted that, although there is a geometrical clear-cut separation between the two regimes, lateral diffusion broadens the signal from the region of OGC into the region of CGC (this effect will increase for shallower sill). Nonetheless, it is clear from Figure 4 that the heat loss is concentrated within the OGC region.

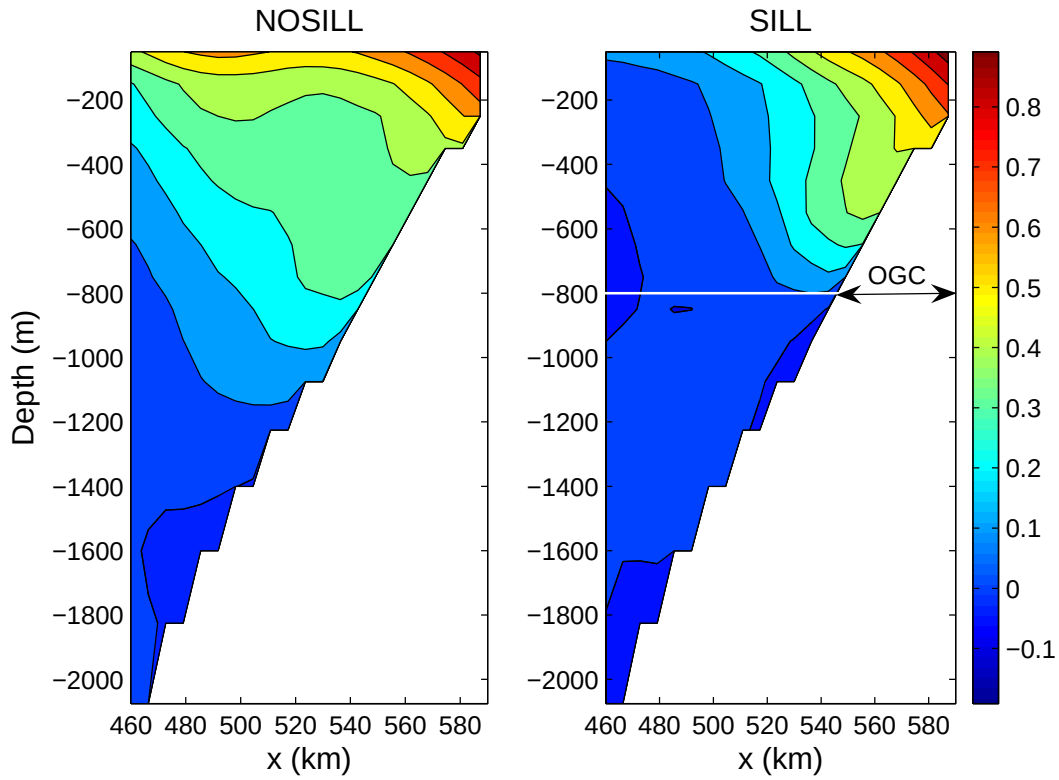


**Figure 4.** Temperature anomalies of the outflowing water relative to the inflow (in °C, contour interval is 0.1 °C) projected in the inflow location, for NOSILL and SILL. White line indicates the sill depth.

### 3.3.3 Sensitivity experiments

A set of experiments has been designed to investigate the sensitivity of water mass properties to variations in the sill configuration. In particular, the experiments differ from SILL only in the depth of the sill, which ranges from 400 m to 1500 m, with increments of 100 m.

We find that the changes in sill depth have an impact on the interior, outflow, and inflowing temperatures (Figure 5). Inflow and outflow temperatures are here calculated by a transport weighted integral as $\int_{x_1}^{x_2}\int_{-H}^{0} vTdxdz \Big/ \int_{x_1}^{x_2}\int_{-H}^{0} vdxdz$ over the sloping-bottom areas indicated in Figure 1.

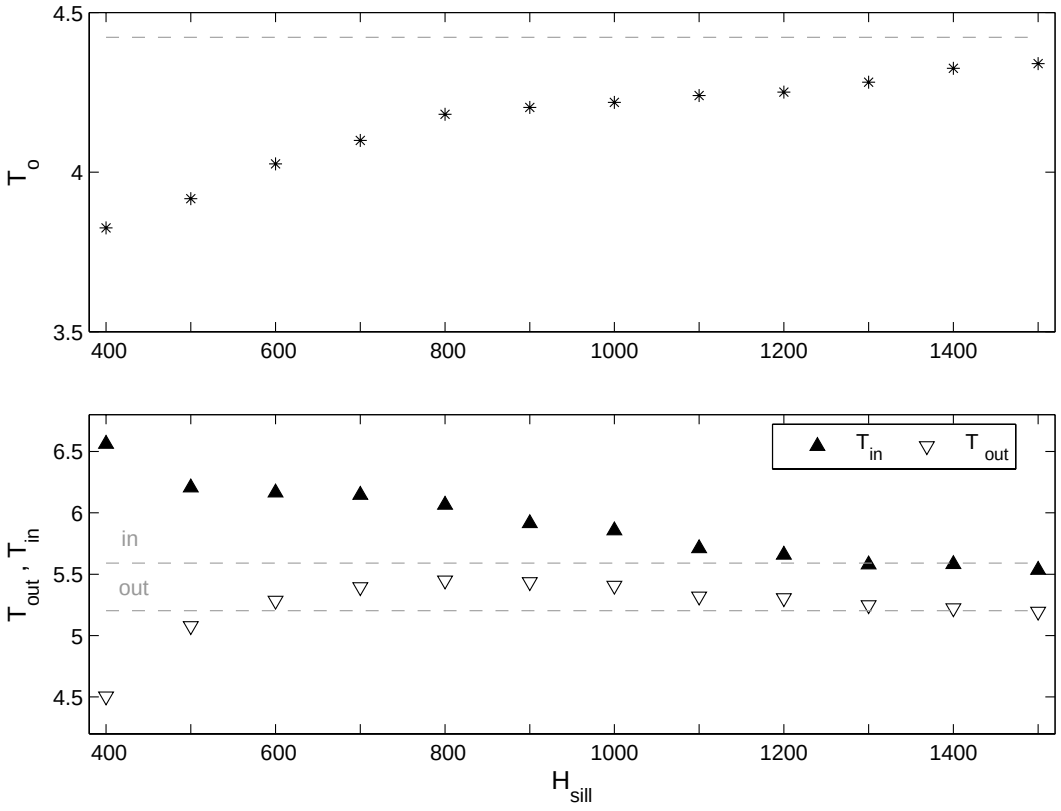


**Figure 5.** Results of the sensitivity experiments: temperatures (in °C) of the interior (upper panel), and of inflow and outflow (transport weighted, lower panel) as function of sill depth, computed over the OGC in the areas indicated in Figure 1. Dashed lines represent NOSILL temperatures.

The interior temperatures are taken at the bottom in the midpoint of the marginal sea. The dense water formed in the interior is colder (denser) the shallower the sill, varying approximately from 3.6 to 4.4 °C. A similar range is found in the outflows, with a decrease down to 4.5 °C. The temperature of the inflows increases with decreasing sill depth: water from the open ocean is stratified, so the colder, deeper water can not enter the basin in presence of the sill. The temperature of the outflowing waters slightly increases for moderate sill depths as a result, even though the interior water is colder. However, the temperature anomaly of the outflow relative to the inflow increases monotonically as sill depth decreases. The shallower the sill, the larger the differences from NOSILL. Accordingly, temperature anomalies become insignificant for deep sills.

## 3.4 Theoretical arguments

We propose here a theoretical argument that relates the water mass properties within the marginal sea to the sill configuration. Our objectives are to gain better insight into the processes responsible for these changes, and to develop a means of quantitatively assessing the impact of the sill. The analytic model is highly idealized, and is an extension of that introduced by Spall (2004) to the case of a basin with a sill.

### *3.4.1 Review of Spall's model*

Spall (2004) proposed a simple parameterization of the baroclinic instability over the sloping bottom in order to provide a theoretical estimate of the density of waters formed in the interior of the marginal sea, of the waters that are exported to the open ocean, and of the net exchange between the marginal sea and the open ocean. The marginal sea is described in terms of three water masses: the waters formed within the interior of the marginal sea, identified by the temperature $T_0$; the waters flowing into the basin from the open ocean, characterized by temperature $T_{in}$, thickness $H_{in}$ (with $H_{in} = dH_{tot}$, where $d$ is a constant of $O(1)$), and velocity $V_{in}$; and the waters flowing out of the basin, with temperature $T_{out}$, thickness $H_{out}$, and velocity $V_{out}$.

The theory is developed by imposing a number of constraints:

1. The net mass transport into the marginal sea is zero: $V_{in}H_{in}L = V_{out}H_{out}L$, where L is the width of the boundary current, taken to be the width of the sloping bottom.

2. The surface heat loss over the marginal sea must be balanced by the advection of heat into and out of the basin: $\frac{\pi R^2 Q}{\rho_0 C_p} = T_{in}V_{in}H_{in}L - T_{out}V_{out}H_{out}L$, where R is the radius of the basin, $Q$ the mean surface heat loss (positive upward), $\rho_0$ the reference density of seawater, and $C_p$ the specific heat capacity of seawater.

3. The flow is in geostrophic balance, such that the inflow is $V_{in} = \frac{\alpha g(T_{in} - T_0)H_{in}}{L\rho_0 f_0}$ where $\alpha$ is the thermal expansion coefficient, $g$ the gravitational acceleration, and $f_0$ the Coriolis parameter.

4. In the interior region, which is assumed to have no mean flow, the annual cooling is balanced by the lateral eddy heat fluxes originating from the boundary current at the edge of the flat bottom: $2\pi R_0 H_{in}\overline{u'T'} = \frac{SQ}{\rho_0 C_p}$, where $R_0$ and $S$ are the radius and area of the interior, respectively. The radii of the basin and its interior are not assumed equal, unlike Spall (2004), because of the larger dimensions of the basin.

5. The lateral eddy heat fluxes are parameterized as $\overline{u'T'} = cV_{in}(T_{in} - T_0)$, where c is a non-dimensional correlation coefficient, linearly related to the eddy efficiency (Spall 2004). Its value has been estimated empirically and theoretically to be $O(10^{-2})$ for flat bottom basin (Visbeck et al 1996; Spall and Chapman 1998), and $O(10^{-3})$ for sloping bottom, where it depends on the bottom slope parameter δ, defined as the ratio of the topographic and isothermal slopes, so that $c = 0.025e^{(2\delta)}$ (Spall 2004). $\delta$ is thus fundamental in quantifying the exchange between the warm boundary current and the interior; for a boundary current flowing cyclonically around the basin in absence of sill $\delta = O(-1)$ (Spall 2004).

Making use of these assumptions and constraints, Spall (2004) is able to relate the properties of the dense water formed, the inflow, and outflow to the basic geometric parameters of the system and the surface heat loss imposed. In particular, the density of the water formed in the

flat-bottom portion of the basin $(T_0)$ relative to the open-ocean temperature $(T_{in})$, is given by:

$$T_{in} - T_0 = \left( \frac{Sf_0 Q}{\alpha g C_p} \right)^{1/2} H_{in}^{-1} \ \varepsilon^{-1/2} \quad (1)$$

and thus, the inflow velocity becomes

$$V_{in} = \frac{1}{L\rho_0} \left( \frac{\alpha g S Q}{f_0 C_p \varepsilon} \right)^{1/2} \quad (2).$$

The parameter ε is a non-dimensional measure of the eddy efficiency, defined in Spall (2004) and Straneo (2006b) as $\varepsilon = 2\pi Rc/L$. In NOSILL, where isotherms intersect the bottom at about the midpoint of the slope and surface on the offshore side of the sloping topography, $\varepsilon = O(0.1)$.

The heat balance in the marginal sea requires the outflowing water to be colder than the inflowing water, and in general warmer than the coldest water formed in the interior of the basin. The temperature decrease between outflow and inflow can be estimated from the balances of heat and mass as function of the fraction of heat fluxed from inflow into the interior by eddies:

$$T_{in} - T_{out} = (T_{in} - T_0)\varepsilon \quad (3).$$

### *3.4.2 Modified theory for a basin with a sill*

The numerical experiments have shown that the introduction of the sill quantitatively impacts the circulation and the properties of the dense water formed, but not the overall system balancing physics of convection in the marginal sea. Thus, we expect the same theoretical arguments developed by Spall (2004) to hold provided one takes into account the modifications introduced by the sill. Physically, the sill blocks deep waters from flowing into and out of the basin, but it also modifies the structure of the boundary current and, hence, the eddy exchanges. Therefore, in terms of the theoretical model's parameters, the sill will affect the thickness of the boundary current, $H_{in}$, and its width, $L$.

We assume here that the boundary current is as deep as the sill

($H_{in} = H_{sill}$), and as wide as the portion of sloping boundary above the sill depth, i.e. the OGC ($L_{sill} = LH_{sill} / H_{tot}$), with $H_{tot}$ the total depth of the basin. The eddy efficiency as function of the sill is altered because of the change in the boundary current width, and its variation is estimated as $\varepsilon_{sill} = 2\pi Rc / L_{sill} = \varepsilon H_{tot} / H_{sill}$, inversely proportional to the sill depth. The change in the isotherms' structure is assumed negligible, so that the parameter c is kept constant. Changes in the geometrical features of the sill affect the efficiency of the lateral eddies: a decrease in $H_{sill}$ increases $\varepsilon_{sill}$, and weakens the transport within the boundary current (as shown in (2)), and hence the exchange between the marginal sea and the open ocean, but strengthens the heat exchange between the boundary current and the interior of the marginal sea (as shown in (1)).

From (1) and (3), the temperature anomalies of the interior and outflowing waters relative to the inflow temperature, $T_{in} - T_0$ and $T_{in} - T_{out}$ are given by

$$T_{in} - T_0 = \left( \frac{Sf_0 Q}{\alpha g C_p} \right)^{1/2} \frac{1}{H_{sill} \ \varepsilon_{sill}^{1/2}} = \left(T_{in} - T_0\right)_{ref} \left( \frac{H_{tot}}{H_{sill}} \right)^{1/2} \qquad (4)$$

and

$$T_{in} - T_{out} = \left(T_{in} - T_0\right)_{sill} \varepsilon_{sill} = \left(T_{in} - T_{out}\right)_{ref} \left( \frac{H_{tot}}{H_{sill}} \right)^{3/2} \qquad (5)$$

The subscript "*ref*" indicates temperature anomalies resulting from a boundary current whose thickness is $H_{in} = dH_{tot}$, where the empirically value $d$ is a constant of $O(1)$; here we chose $d = 0.65$.

### *3.4.3 Comparison with numerical model*

We first evaluate the validity of the analytical model by comparing the interior and outflowing temperature predictions (4) and (5) with the numerical experiments. The temperature of the waters formed in the interior of the marginal sea and the temperature of the outflow are calculated for each of the numerical simulations and compared to the theoretical estimate. The theory does not predict the inflow

temperatures. The good agreement between theory and model solutions, with a correlation of 0.99 (0.97) and a least square line of slope 1.22 (1.19) for $T_0$ $(T_{out})$, confirms the theory's applicability to the sill case (Figure 6). It is worth to note that the anomaly $T_{out} - T_0$ shows that the outflowing water is always warmer than the interior water, is a maximum for $H_{sill} \approx 700m$, but its temperature approaches $T_0$ for $H_{sill}/H_{tot} << 1$.

To better understand how the two mechanisms (blocking and change in the stability) affect the interior-water properties, we use the theory to investigate their impact separately. First, we consider the effect of blocking alone by neglecting the change in the boundary current width (and $\varepsilon$). The changes in $T_0$ and $T_{out}$ are hence due the variation of the flow thickness alone, while ε is kept constant and equal to the NOSILL case ($\varepsilon =$ 0.11). From (4) and (5), the theory predicts the variations in $T_0$ and $T_{out}$ to be inversely proportional to $H_{sill}$ (Figure 6, curves labelled $\varepsilon$ constant): $T_{in} - T_0 = (T_{in} - T_0)_{ref}(H_{tot}/H_{sill})$ and $T_{in} - T_{out} = (T_{in} - T_{out})_{ref}(H_{tot}/H_{sill})$, respectively. If we compare the prediction of the interior temperature to the numerical solutions, it is clear that though the change is of the same sign (colder waters for shallower sills); the predictions with $\varepsilon$ fixed yield an interior that is too cold and thus an outflow that is too warm.

The sill also affects the boundary current stability. Next, we consider the impact on $T_0$ and $T_{out}$ of the change in the eddy efficiency alone: let $H_{in}$ be constant while ε is computed as a function of $L_{sill}$. According to equation (4), $T_0$ will increase for shallower sills, as $H_{sill}^{1/2}$: $T_{in} - T_0 = (T_{in} - T_0)_{ref}(H_{sill}/H_{tot})^{1/2}$. This change is of the opposite sign of the blocking effect and is associated with a progressively more unstable boundary current which is able to release more heat to the interior. As $H_{sill}$ decreases, the temperature interior-boundary current difference decreases since eddies exchange heat much more efficiently. The increase in the eddy flux with shallowing sill depth consequently results in a decrease in the outflow temperature, or an increase in $T_{in}$-$T_{out}$ From (5), the variation in $T_{out}$ is inversely proportional to $H_{sill}^{1/2}$, (Figure 6, curves labelled $H_{in}$ fixed): $T_{in} - T_{out} = (T_{in} - T_{out})_{ref}(H_{tot}/H_{sill})^{1/2}$.

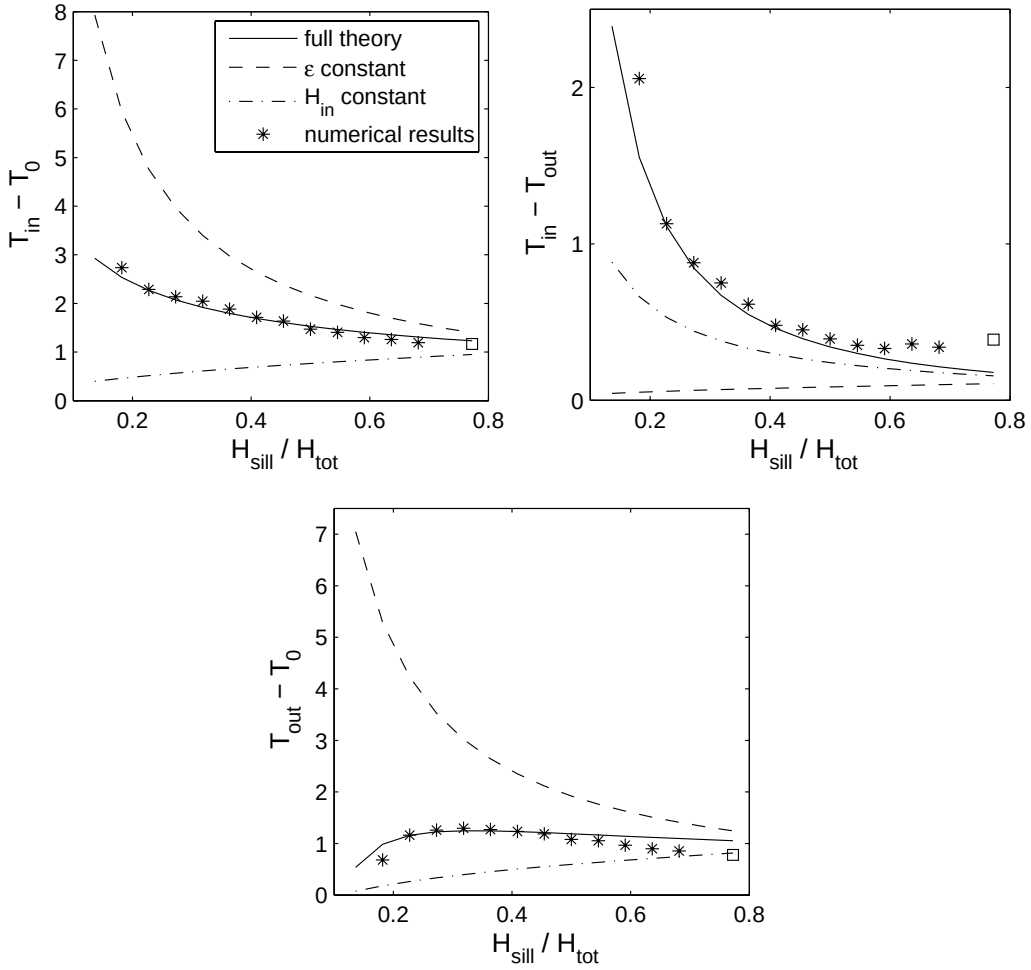


**Figure 6.** Comparison between the temperature anomalies (in °C) of the interior ($T_0$, upper-left panel) and outflowing waters ($T_{out}$, upper-right panel) relative to the inflow temperature ($T_{in}$) computed from the set of numerical simulations (stars) and from the theoretical calculations as function of $H_{in}$ and $\varepsilon$. Comparison for $T_{out} - T_0$ (in °C) is the lower panel. Squares indicate numerical NOSILL calculations.

These results indicate that, while the greatest impact of the sill is to limit the net heat transport into the basin, the interior (outflow) is not as cold (warm) as it would have been due to the blocking effect alone. Instead, the reduction of the width of the heat transporting part of the boundary current structure due to the sill results in destabilizing the boundary current and increasing the interior/boundary current heat exchange. The net impact of the sill is thus a colder interior and a colder

outflow (Figures 5 and 6). The two effects, decrease of $H_{in}$ and increase of $\varepsilon$, partly offset each other.

### *3.4.4 Change around the basin*

In the dynamics described above, the cooling in the interior of the marginal sea is balanced by release of heat from the boundary current. Hence, because of the exchange between the two regions, this current is warmer than the interior, and its temperature decreases from inflow to outflow; so that $T_{in} > T_{out} > T_0$. The temperature at any given point around the basin $(l)$ can be obtained by $T(l) = T_{in} + T_d(l)$, where $T_d$ is the temperature decay along the perimeter.

Straneo (2006b) provided an estimate of the change in temperature around the basin as a function of the parameters of the system. With the assumptions that the changes in the boundary current are small ($T_d \ll T_{in} - T_0$), so that the amount of heat exchanged by eddies is relatively smaller than the heat transported around the basin, we obtain a linear analytical solution

$$T_d(l) = (T_{in} - T_0)(1 - e^{-2l\varepsilon/\pi R}).$$

The theory predicts an exponential decay that decreases as the eddy exchange goes to zero. The decay rate around the basin found in the numerical model runs is compared to the analytical prediction in Figure 7. In order to highlight the differences between shallow and deep sills, we use the simulations with a sill at 500 and 1500 m. The temperature in the boundary current (over the OGC) decays along the perimeter much more rapidly in the shallow sill case than in the deep one, and the interior/boundary temperature difference $T_{in} - T_0$ is initially much larger. The trend of these decays compares well with a least square exponential fit, suggesting that an exponential decay is a good representation of the numerical decay rate (Figure 7). The slope of the least square exponential fit is decay rate is compared to $\varepsilon_{sill}$ for different sill depths. The decay rate increases approximately linearly for decreasing sill depth (i.e., increasing $\varepsilon_{sill}$) with a slope of $O(1)$ (Figure 7). Although the comparison is not very close for deep sills, there is general agreement between the changes of the decay rate with sill depth and the linear theory.

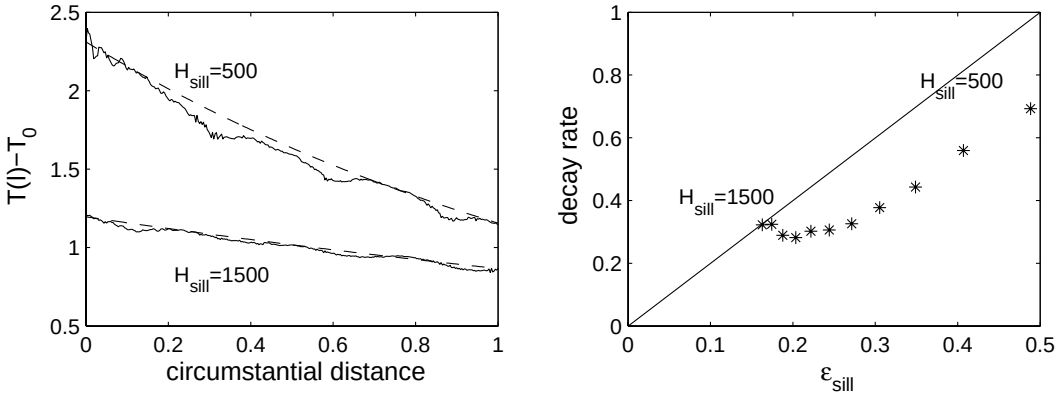


**Figure 7.** Decay of the interior/boundary current temperature difference $T(l) - T_0$ (in °C, with $T(l)$ integrated over the OGC) as a function of perimeter (solid lines), and the least square exponential fits to the model data for simulations with a sill at 1500 m and 500 m (dashed lines, left panel). Comparison between $\varepsilon_{sill}$ and the slope of least square fit to the exponential decay rate for the set of numerical calculations (the 400 m deep sill is not shown).

## 3.5 Summary and conclusions

Both numerical and analytical models have been used to analyze the large-scale circulation in a semi-enclosed convective basin subject to a basin-scale surface cooling. The key aspect of the model configuration is the introduction of a sill in the narrow strait connecting the basin to the open ocean.

The general characteristics of the circulation with and without a sill are alike: the net heat loss from the marginal sea to the atmosphere is balanced by lateral advection from the open ocean through the strait through a warm boundary current that moves cyclonically around the basin. The key process that determines the properties of the water mass transformation in the marginal sea is the interaction between the boundary current and the interior of the marginal sea; these exchanges are due to mesoscale eddies, and are controlled by baroclinic instabilities of the boundary current. In the absence of a sill, the structure of the boundary current and its instability are set by the bottom slope, but in basins with a sill they are also influenced by its depth; so that the properties of the flows in and out of the basin, and consequently of the

deep water formed in the interior, are modified accordingly. Numerical simulations have indeed shown that some important differences result when a sill is introduced: the interior becomes colder; the outflow temperature decreases; the boundary current structure becomes narrower and shallower; mean advection of heat is mainly confined over the open geostrophic contours (at and above the sill level). Furthermore, in the presence of a sill the circulation takes longer to reach a steady-state. The magnitude of the sill influence is a function of its depth. When the sill is introduced the transport of warm water into the marginal sea is limited (because of the blocking effect) with a consequent reduction of the temperature of the water formed within the basin. Theoretical analysis provides further insight into the dynamics at play: the blocking effect is only one part of the sill impact on the interior water. A second effect due to the sill is the modification of the width of the inflow that becomes more unstable and so more efficient in transmitting heat to the interior. As a result, the interior is not as cold as it would be by the blocking alone. On the other hand, the outflow is notably colder than in the absence of a sill. This result highlights how important the topographic constraint is in setting both the amount of warm water that can be transported into the marginal sea, and the interior/boundary current exchanges.

### *3.5.1 Relevance for the Nordic Seas*

Our results may provide a better understanding of some aspects of the northward transport of warm water and the formation of deep water in the North Atlantic-Nordic Seas system. Blindheim and Østerhus (2005) describe the large-scale circulation in the Nordic Seas in details. The near surface circulation of the Nordic Seas is basically cyclonic: warm and saline Atlantic water flows northward, approximately in the upper 700 m, in the Norwegian Atlantic Current on the eastern side of the basin; a flow of cold and fresh water moves southwards in the East Greenland Current and follows the Greenland continental slope. In the center of the basin there are cyclonic cells linked to the bottom topography. The two basins are connected through the Denmark Strait (620 m deep), the Iceland-Faroe Ridge (500 m deep), and the Faroe-Shetland Channel (850 m deep). North of the sill the Atlantic water (with temperature of about 7 °C) flows with a thickness apparently fixed by the sill depth (Blindheim and Østerhus 2005). This current is progressively cooled and freshened as it proceeds through the basin (by both the winter heat loss to the atmosphere and the exchange with the

interior), so that the Nordic Seas overflow is cold and dense, although it does not include the coldest and deepest water formed in the interior, but rather derives from the boundary current flowing above sill depth (Mauritzen 1996a,b). This scenario is well predicted by our models: the interior is always colder (denser) that the overflow, which comprises waters carried in the boundary current. This perspective disagrees with a traditional point of view that considers the overflows to be the result of deep convection in the internal gyres of the Nordic Seas (e.g., Aagaard et al. 1985, Hopkins 1991).

This study neglects some fundamental aspects of the realistic Nordic Seas scenario. The effect of freshwater fluxes is disregarded in our models; for example, the interaction with the Arctic Ocean and the export of freshwater through Fram Strait might change the characteristics of the boundary current (Broström and Ferrow 2007). We also ignore the effect of wind forcing on the circulation, which has undoubtedly an important role in the variability of the exchanges between the North Atlantic and the Nordic Seas (Furevik and Nilsen 2005). Nonetheless, by focusing on this simpler system, we feel that we have been able to isolate the primary effect of a sill on the buoyancy-forced circulation within a marginal sea and its exchange with the open ocean.

**Acknowledgments:** DI was supported by the *Polar Ocean Climate Processes* (ProClim) project funded by the *Norwegian Research Council*. FS was supported by a visiting scientist fellowship from the *Bjerknes Centre for Climate Research (Bergen, Norway).* Support for MAS was provided by *NSF Office of Polar Programs Grant 0421904 and NSF Ocean Sciences Grant 0423975*.

## References

Aagard, K., J.H. Swift, and E.C. Carmack, 1985: Thermohaline circulation in the arctic Mediterranean seas. *Journal of Geophysical Research*, 90, 4833-4846.

Blindheim, J., and S. Østerhus, 2005: The Nordic Seas, Main Oceanographic Features. In *The Nordic Seas: An integrated perspective*, H. Drange, T.M. Dokken, T. Furevik, R. Gerdes, and W. Berger, eds., American Geophysical Union, Washington DC, USA, 11-38, AGU Monograph 158.

Broström, G. and A. Ferrow, 2007: Dual buoyancy forcing in semi-enclosed seas: An idealized study of the Arctic Mediterranean. *Journal of Marine Research*, submitted.

Canuto, V. M., A. Howard, P. Hogan, Y. Cheng, M.S. Dubovikov, and L.M. Montenegro, 2004. Modeling ocean deep convection. *Ocean Modelling,* 7, 75-95.

Furevik, T. and J.E.Ø. Nilsen, 2005: Large-Scale Atmospheric Circulation Variability and its Impacts on the Nordic Seas Ocean Climate - a Review. In *The Nordic Seas: An integrated perspective*, H. Drange, T.M. Dokken, T. Furevik, R. Gerdes, and W. Berger, eds., American Geophysical Union, Washington DC, USA, 105-136, AGU Monograph 158.

Hopkins, T.S., 1991: The GIN Sea - a synthesis of its physical oceanography and literature review 1972-1985. *Earth Science Reviews*, 30, 175-318.

IPCC, 2001: Climate Change 2001: The Scientific Basis - Contribution of Working Group I to the Third Assessment Report of the Intergovernmental Panel on Climate Change. Cambridge University Press. 881 pp.

Jones, H., and J. Marshall, 1993. Convection with rotation in a neutral ocean. A study of open-ocean deep convection. *Journal of Physical Oceanography*, 23, 1009-1039.

LabSea Group, 1998: The Labrador Sea Deep Convection Experiment. *Bullettin of the American Meteorological Society*, 79, 2033-2058.

Marotzke, J., 2000: Abrupt climate change and thermohaline circulation: Mechanisms and predictability. *Proceedings of the National Academy of Sciences (U.S.A.)*, 97, 1347-1350.

Marshall, J., C. Hill, L. Perelman, and A. Adcroft, 1997a: Hydrostatic, quasi-hydrostatic, and nonhydrostatic ocean modeling. *J. Geophysical Res.*, 102(C3), 5733-5752.

Marshall, J., A. Adcroft, C. Hill, L. Perelman, and C. Heisey, 1997b: A finite-volume, incompressible Navier Stokes model for studies of the ocean on parallel computers. *Journal of Geophysical Research.*, 102(C3), 5753-5766.

Marshall, J., and F. Schott, 1999: Open ocean deep convection: observations, theory and models. *Reviews of Geophysics*, 37, 1-64.

Mauritzen, C., 1996a: Production of dense overflow waters feeding the North Atlantic across the Greenland-Scotland Ridge. Part 1: Evidence for a revised circulation scheme. *Deep-Sea Research* I, 43, 769-806.

Mauritzen, C., 1996b: Production of dense overflow waters feeding the North Atlantic across the Greenland-Scotland Ridge. Part 2: An inverse model. *Deep-Sea Research I*, 43, 807-835.

Rahmstorf, S., 2002: Ocean circulation and climate during the past 120.000 years. *Nature*, 419, 207-214.

Roberts, M. J., and R. A. Wood, 1997: Topographic sensitivity studies with a Bryan-Cox-Type ocean model. *Journal of Physical Oceanography,* 27, 823-836.

Spall, M. A., 2003: On the thermohaline circulation in flat bottom marginal seas. *Journal of Marine Research*, 61, 1-25.

Spall, M. A., 2004: Boundary currents and water mass transformation in marginal seas. *Journal of Physical Oceanography*, 34, 1197-1213.

Spall, M. A., 2005: Buoyancy-forced circulations in shallow marginal seas. *J. Mar. Res.* 63, 729-752.

Spall, M. A., and D. C. Chapman, 1998: On efficiency of baroclinic eddy heat transport across narrow fronts. *Journal of Physical Oceanography,* 28, 2275-2287.

Straneo, F., 2006a: Heat and Freshwater Transport through the Central Labrador Sea. *Journal of Physical Oceanography,* 36, 606-628.

Straneo, F., 2006b: On the connection between dense water formation, overturning, and poleward heat transport in a convective basin. *Journal of Physical Oceanography*, 36, 1822-1840.

Visbeck, M., J. Marshall, and H. Jones, 1996: Dynamics of isolated convective regions in the ocean. *Journal of Physical Oceanography,* 26, 1721-1734.

Walin G., G. Broström, J. Nilsson, and O. Dahl, 2004: Baroclinic boundary currents with downstream decreasing buoyancy; a study of an idealized Nordic Seas system. *Journal of Marine Research*, 62, 517-543.